Journal of Sound and Vibration 329 (2010) 2205–2217

Contents lists available at ScienceDirect

Journal of Sound and Vibration

journal homepage: www.elsevier.com/locate/jsvi

Amplitude reduction of parametric resonance by dynamic vibration absorber based on quadratic nonlinear coupling

Hoonhee Jo [a], Hiroshi Yabuno [b,*]

[a] Graduate School of Systems and Information Engineering, University of Tsukuba, Tsukuba 305-8573, Japan
[b] Department of Mechanical Engineering, Faculty of Science and Technology, Keio University, Yokohama 223-8522, Japan

ARTICLE INFO

Article history:
Received 5 August 2008
Received in revised form
15 December 2009
Accepted 2 January 2010
Handling Editor: L.G. Tham
Available online 27 January 2010

ABSTRACT

The paper proposes an amplitude reduction method for parametric resonance with a new type of dynamic vibration absorber utilizing quadratic nonlinear coupling. A main system with asymmetric nonlinear restoring force and harmonic excitation causes parametric resonance in the system. In contrast with autoparametric vibration absorber, the natural frequency of the vibration absorber is tuned to be in the neighborhood of twice that of the main system. For such a vibration absorber, we investigate the effect on the amplitude reduction for a parametrically excited main system. Analytical results using the method of multiple scales show that the amplitude of parametric resonance is reduced by the effect of the vibration absorber. The experimental results by a simple apparatus indicate that the parametric resonance is stabilized by the effects of both vibration absorber and Coulomb friction of the main system. Moreover, numerical results considering the Coulomb friction of the main system show that the amplitude of parametric resonance becomes close to zero by the proposed vibration absorber.

1. Introduction

Principal parametric resonance occurs in systems having time-varying coefficients through pitchfork bifurcation in the case when the excitation frequency is in the neighborhood of twice the natural frequency of the system. The book written by Nayfeh and Mook [1] showed the mechanism of parametric resonance and history of research concerning this one, i.e., Faraday who has been the first to recognize the phenomenon of parametric resonance and Melde who performed the first serious experiments on parametric resonance. From physical and engineering points of view, the parametric resonance has been attractive, and many researches on the phenomena and their utilization have been continuously performed until now. Pratiher et al. [2] investigated parametric instabilities of a cantilever beam with magnetic field and axial load. Huang and Kuang [3] studied the parametric resonance instabilities in a drilling process. Shaw and Baskaran [4] investigated the use of parametric resonance to improve filtering characteristics in microelectromechanical filters. Piccardo and Tubino [5] analyzed the excessive lateral sway motion caused by crowds walking across footbridges using parametric excitation mechanism. Racz and Scott [6] investigated the parametric instability in a finite-length rotating cylinder subjected to periodic axial compression by small sinusoidal oscillations of the piston.

In addition to the analysis of parametric resonance, control methods are also studied. Mustafa and Ertas [7] dealt with the dynamics and bifurcations of a large flexible column with a tip mass-pendulum under parametric excitation. They

* Corresponding author.
E-mail address: yabuno@mech.keio.ac.jp (H. Yabuno).

0022-460X/$ - see front matter © 2010 Elsevier Ltd. All rights reserved.
doi:10.1016/j.jsv.2010.01.006

revealed that the column amplitude shows saturation and the pendulum acts as a vibration absorber in the case when the natural frequency of the pendulum is a half that of the column. Yabuno et al. [8] stabilized the parametric resonance by exploiting the effect of a low static friction acting at the pivot point of attachment of a pendulum to the beam tip. The low static friction acts to shift the unstable region where the parametric resonance is activated in the amplitude–frequency plane. Lacarbonara et al. [9] developed a control strategy using open-loop resonance cancellation for a hinged–hinged shallow arch, which is parametrically excited by longitudinal end-displacement. Autoparametric vibration absorber [10] is well known as a nonlinear vibration absorber (see [11,12] for the comprehensive survey of the characteristics of control method). While the autoparametric vibration absorber is applicable to control of primary resonance, Yabuno et al. showed that an autoparametric vibration absorber cannot stabilize the parametric resonance, but the autoparametric coupling produces chaotic motions in the main system. Furthermore, they proposed an active actuation pendulum as the vibration absorber which is based on open-loop resonance cancellation [13]. In order to overcome such a drawback of the autoparametric vibration absorber, we proposed a new type of nonlinear dynamics vibration absorber in [15], and theoretically and experimentally confirmed the validity for the primary resonance. In this paper, we investigate the effectiveness for parametric resonance.

Contrast with the conventional nonlinear vibration absorber, i.e., autoparametric vibration absorber in which the natural frequency of the absorber is tuned to be a half the natural frequency of the main system, the natural frequency of the proposed absorber is tuned to be twice the natural frequency of the main system. We introduce a new geometric configuration of vibration absorber in order to induce quadratic nonlinear coupling. The pendulum-type vibration absorber is connected to the main system through a link and excited at twice the response frequency of the main system. Because the usual autoparametric vibration absorber has the trivial steady state, the motion can be trapped by Coulomb friction acting on the absorber (for example, the effect of pendulum-type vibration absorber is vanished by the Coulomb friction at the pivot point of the pendulum) and it cannot occasionally work as the vibration absorber. On the contrary, because the proposed vibration absorber has no trivial steady state, it works independent of the Coulomb friction. In this paper, the validity of the proposed absorber for the parametric resonance is confirmed analytically using the method of multiple scales and experimentally using a simple apparatus. Analytical results show that the steady-state amplitude of parametric resonance is reduced by the effect of the vibration absorber. Furthermore, from the experimental results, we indicate that the parametric resonance is stabilized by the effect of both vibration absorber and Coulomb friction, which exists inherently in the main system. Numerical results considering Coulomb friction of the main system by Runge–Kutta method show that the amplitude of parametric resonance becomes close to zero.

2. Stabilization of parametric resonance

2.1. Equation of motion

We consider a main system subjected to magnetic forces as a nonlinear restoring force is shown in Fig. 1 [14]. The dynamics is widely corresponding to those of the systems subjected to asymmetric nonlinear restoring force [14]. We set the origin O of a static Cartesian coordinate x–y–z at a point p on the main system in the static equilibrium state. The mass M can be moved freely only in the y-direction and its motion is expressed by the displacement y of the point p from the origin O in the y-direction. We move magnet A as $y_0 = a_e \cos Nt$ in the y-direction as the external excitation. The repulsive force by same magnetic pole acts between magnet B' on the main system and fixed magnet A', and between magnet B on the main system and moved magnet A. We propose the following absorber [15], which oscillates with twice the response

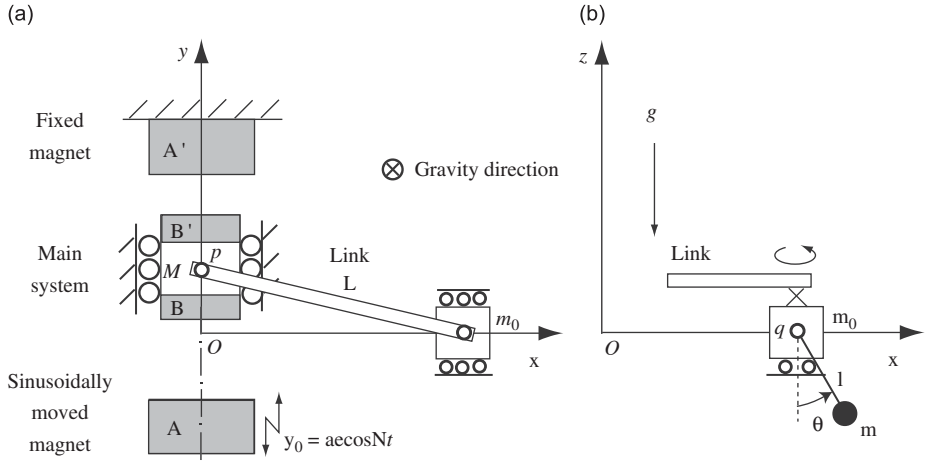

Fig. 1. Analytical model with nonlinear dynamic vibration absorber. (a) Main system with absorber, (b) absorber.

frequency of the main system. A mass m_0 is connected to the point p on the main system through a link and can be moved freely only in the x-direction and is excited at twice the response frequency of the main system. A pendulum with tip mass m is attached vertically to the mass m_0 as a nonlinear dynamic vibration absorber and its motion is expressed in terms of the angle θ about the point q on the z–x plane. In contrast with autoparametric vibration absorber, the pendulum is always excited by the motion of the main system and is not trapped by the Coulomb friction, which exists at the pivot point.

The equation of motion of the main system without absorber is obtained [15] as follows:

$$M\frac{d^2y}{dt^2} = -(K_{R1}+K_{L1})y-(K_{R2}-K_{L2})y^2-(K_{R3}+K_{L3})y^3+K_{R1}y_0+2K_{R2}y_0y-K_{R2}y_0^2+3K_{R3}y_0y^2-3K_{R3}y_0^2y+K_{R3}y_0^3. \quad (1)$$

The repulsive force F_B acting on the magnet B by the magnet A in Fig. 1(a) is calculated by Coulomb's law. The coefficients of linear, quadratic, and cubic terms by Taylor expansion of F_B with respect to y are K_{R1}, K_{R2}, and K_{R3}, respectively. Similarly, the repulsive force $F_{B'}$ acting on the magnet B' by the magnet A' is calculated by Coulomb's law. The coefficients of linear, quadratic, and cubic terms by Taylor expansion of $F_{B'}$ with respect to y are K_{L1}, K_{L2}, and K_{L3}, respectively. The derivation of Eq. (1) and the equation including the effect of the absorber, Eqs. (2) and (3) mentioned later, is described in [15].

The equation of motion of the main system and the absorber in the case when an absorber is connected to the main system through a link is obtained [15] up to cubic terms as follows:

$$\left\{M+\frac{(m_0+m)}{L^2}y^2\right\}\frac{d^2y}{dt^2}+\frac{(m_0+m)}{L^2}y\left(\frac{dy}{dt}\right)^2+\frac{ml}{L}\frac{d^2\theta}{dt^2}y+(K_{R1}+K_{L1})y+(K_{R2}-K_{L2})y^2+(K_{R3}+K_{L3})y^3$$
$$=K_{R1}y_0+2K_{R2}y_0y-K_{R2}y_0^2+3K_{R3}y_0y^2-3K_{R3}y_0^2y+K_{R3}y_0^3, \quad (2)$$

$$ml^2\frac{d^2\theta}{dt^2}+mgl\theta = -ml\frac{d^2y_0}{dt^2}\theta-\frac{ml}{L}\left\{\left(\frac{dy}{dt}\right)^2+y\frac{d^2y}{dt^2}\right\}+\frac{mgl\theta^3}{6}. \quad (3)$$

2.2. Parametric resonance in the case without control

First, we analyze the parametric resonance in the case without control, i.e., absorber is not in action and then θ is fixed to zero, using the method of multiple scales. The dimensionless equation of motion of Eq. (1) normalized by y_{st} and $T=1/\sqrt{(K_{R1}+K_{L1})/M}$ is

$$\ddot{y}+2\mu_1\dot{y}+(1+2a_ek_{R2}\cos\nu t)y+\alpha_2y^2+\alpha_3y^3 = a_ek_{R1}\cos\nu t-a_e^2k_{R2}\cos^2\nu t+a_e^3k_{R3}\cos^3\nu t-3a_e^2k_{R3}\cos^2\nu ty+3a_ek_{R3}\cos\nu ty^2, \quad (4)$$

where the dot indicates the derivative with respect to the dimensionless time t^*, and μ_1 is the damping coefficient of the main system. Also, α_2 and α_3 are the coefficients of Taylor expansion of the magnetic force with respect to y^{*2} and y^{*3}, respectively. The asterisk $(*)$ is omitted for simplification. The dimensionless parameters in Eq. (4) are as follows:

$$t^*=\frac{t}{T},\quad y^*=\frac{y}{y_{st}},\quad \nu=NT,\quad \alpha_2=\frac{(K_{R2}-K_{L2})y_{st}}{(K_{R1}+K_{L1})},\quad \alpha_3=\frac{(K_{R3}+K_{L3})y_{st}^2}{(K_{R1}+K_{L1})},$$

$$k_{R1}=\frac{K_{R1}}{K_{R1}+K_{L1}},\quad k_{R2}=\frac{K_{R2}y_{st}}{(K_{R1}+K_{L1})},\quad k_{R3}=\frac{K_{R3}y_{st}^2}{(K_{R1}+K_{L1})},\quad a_e^*=\frac{a_e}{y_{st}}. \quad (5)$$

The values of the dimensionless parameters used in the theoretical analyses correspond to those in the subsequent experiment: $\mu_1=0.0155$, $a_e^*=0.1212$, $k_{R1}=0.507566$, $k_{R2}=-0.442311$, $k_{R3}=0.2576$, $\alpha_2=-0.0432638$, $\alpha_3=0.512554$.

In Eq. (4), the damping force is assumed to be small. Using the order parameter $0<\varepsilon\ll 1$, we put $\mu_1=\varepsilon\hat{\mu}_1(\hat{\mu}_1=O(1))$, and the excitation amplitude of magnet A is assumed to be small compared with the gap between magnets A and B in the initial static equilibrium state and set as $a_e^*=\varepsilon\hat{a}_e(\hat{a}_e=O(1))$. We define a detuning parameter $\sigma=\varepsilon\hat{\sigma}(\hat{\sigma}=O(1))$ such as $\nu=2+\varepsilon\hat{\sigma}$ to express the nearness of the parametric resonance and introduce the multiple time scales of $t_0=t$, $t_1=\varepsilon^{1/2}t$, and $t_2=\varepsilon t$. We expand y as

$$y=\varepsilon^{1/2}y_1+\varepsilon y_2+\varepsilon^{3/2}x_3 \quad (6)$$

and apply the method of multiple scales. Then, the first-order approximate solution of Eq. (4) is obtained as

$$y=a_1\cos\left(\frac{\nu}{2}t-\theta_1\right)+O(\varepsilon), \quad (7)$$

where $a_1=\varepsilon^{1/2}\hat{a}_1$. Time variations of the amplitude and phase are governed with

$$\frac{da_1}{dt}=-\mu_1a_1-\left(\frac{k_{R2}}{2}-\frac{k_{R1}\alpha_2}{2(1-\nu^2)}\right)a_e\sin2\theta_1a_1, \quad (8)$$

$$a_1\frac{d\theta_1}{dt}=\frac{\sigma}{2}a_1-\left(\frac{k_{R2}}{2}-\frac{k_{R1}\alpha_2}{2(1-\nu^2)}\right)a_e\cos2\theta_1a_1-\frac{1}{24}(9\alpha_3-10\alpha_2^2)a_1^3. \quad (9)$$

For the steady-state solution, letting $da_1/dt = d\theta_1/dt = 0$, and Eqs. (8) and (9) are combined into as

$$a_{1st} = \sqrt{\frac{12\sigma \pm 24\sqrt{\left(\frac{k_{R2}}{2} + \frac{k_{R1}\alpha_2}{2(\nu^2-1)}\right)^2 a_e^2 - \mu_1^2}}{9\alpha_3 - 10\alpha_2^2}}. \tag{10}$$

Fig. 2 shows the frequency response curve in the case when absorber is not in action.

2.3. Amplitude reduction of parametric resonance by proposed absorber

We analyze the dynamics of the main system in the case with control, i.e., absorber is in action, using the method of the multiple scales. Normalized equations of motion of Eqs. (2) and (3) by y_{st} and $T = 1/\sqrt{(K_{R1}+K_{L1})/M}$ are

$$\begin{aligned}\ddot{y} + 2\mu_1\dot{y} + (1 + 2a_e k_{R2}\cos\nu t)y + \alpha_2 y^2 + \alpha_3 y^3 = {} & -c_1(y\dot{y}^2 + y^2\ddot{y}) - c_2\ddot{\theta}y + a_e k_{R1}\cos\nu t - a_e^2 k_{R2}\cos^2\nu t \\ & + a_e^3 k_{R3}\cos^3\nu t - 3a_e^2 k_{R3}\cos^2\nu t y + 3a_e k_{R3}\cos\nu t y^2,\end{aligned} \tag{11}$$

$$\ddot{\theta} + 2\mu_2\dot{\theta} + \omega_\theta^2\theta = -c_3 y\ddot{y} - c_3\dot{y}^2 + c_4 a_e\cos\nu t\theta - \tfrac{1}{6}\omega_\theta^2\theta^3, \tag{12}$$

where the dot indicates the derivative with respect to the dimensionless time t^*, and μ_2 is the damping coefficient of the absorber, respectively. Also, c_1, c_2, c_3, and c_4 are the coefficients determined by system parameters, which are expressed as follows:

$$c_1 = \frac{m^*_{total}}{\Lambda^2}, \quad c_2 = \frac{m^* l^*}{\Lambda}, \quad c_3 = \frac{1}{\Lambda l^*}, \quad c_4 = \frac{\nu^2}{l^*}, \tag{13}$$

where $m^*_{total} = (m+m_0)/M$, $m^* = m/M$, $l^* = l/y_{st}$, and $\Lambda = L/y_{st}$. The main system and the absorber are nonlinearly coupled through term $-c_2\ddot{\theta}y$ in Eq. (11) and terms, $-c_3 y\ddot{y}$ and $-c_3\dot{y}^2$, in Eq. (12). Then, in Eq. (12), the motion of the absorber is excited by the terms $-c_3 y\ddot{y}$ and $-c_3\dot{y}^2$, which act as equivalent external excitation to the absorber. When the natural frequency of the absorber is tuned to be close to twice the natural frequency of the main system, i.e., $\omega_\theta \approx 2$, the resonance in absorber occurs by the terms, $-c_3 y\ddot{y}$ and $-c_3\dot{y}^2$, in Eq. (12) because the frequency of these terms is near 2. Through the quadratic nonlinear coupling, the energy of the main system is transferred to the absorber and finally the resonance amplitude of the main system is reduced.

The damping force of the absorber is assumed to be small. Using the order parameter $0 < \varepsilon \ll 1$, we put $\mu_2 = \varepsilon\hat{\mu}_2 (\hat{\mu}_2 = O(1))$, and we define a detuning parameter $\rho = \varepsilon^{1/2}\hat{\rho} (\hat{\rho} = O(1))$ such as $\omega_\theta = 2 + \varepsilon^{1/2}\hat{\rho}$ to express the tuning of the natural frequency of the absorber. We expand y and θ as

$$y = \varepsilon^{1/2}y_1 + \varepsilon y_2 + \varepsilon^{3/2}y_3, \tag{14}$$

$$\theta = \varepsilon^{1/2}\theta_1 + \varepsilon\theta_2 + \varepsilon^{3/2}\theta_3. \tag{15}$$

By introducing multiple time scales of $t_0 = t$, $t_1 = \varepsilon^{1/2}t$, and $t_2 = \varepsilon t$, we obtain the following equations by equating the coefficients of $O(\varepsilon^{1/2})$, $O(\varepsilon)$, and $O(\varepsilon^{3/2})$ to zero.

Order $\varepsilon^{1/2}$

$$D_0^2 y_1 + y_1 = 0, \tag{16}$$

$$D_0^2\theta_1 + \omega_\theta^2\theta_1 = 0. \tag{17}$$

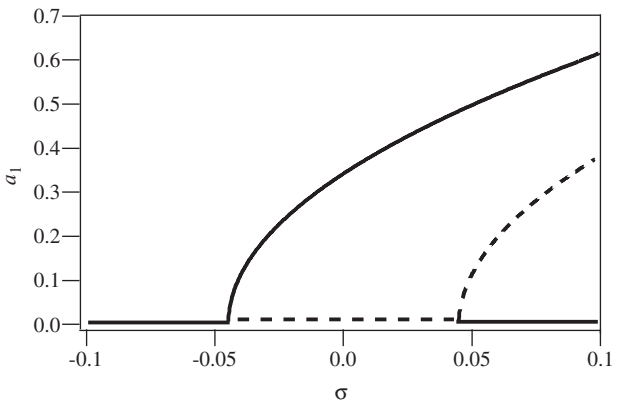

Fig. 2. Frequency response curve in case absorber is not in action: —— stable, – – – unstable.

Order ε

$$D_0^2 y_2 + y_2 = -2D_0D_1y_1 - \alpha_2 y_1^2 - c_2 y_1 D_0^2\theta_1 + \hat{a}_e k_{R1}\cos\nu t_0, \tag{18}$$

$$D_0^2\theta_2 + \omega_\theta^2\theta_2 = -2D_0D_1\theta_1 - c_3 y_1 D_0^2 y_1 - c_3(D_0y_1)^2. \tag{19}$$

Order $\varepsilon^{3/2}$

$$\begin{aligned} D_0^2 y_3 + y_3 = {} & -2D_0D_1y_2 - D_1^2y_1 - 2D_0D_2y_1 - 2\hat{\mu}_1 D_0y_1 - 2\hat{a}_e k_{R2}\cos\nu t_0 y_1 - 2\alpha_2 y_1 y_2 \\ & - \alpha_3 y_1^3 - c_1 y_1 (D_0y_1)^2 - c_1 y_1^2 D_0^2 y_1 - c_2 y_1 D_0^2\theta_1 - 2c_2 y_1 D_0D_1\theta_1, \end{aligned} \tag{20}$$

$$\begin{aligned} D_0^2\theta_3 + \omega_\theta^2\theta_3 = {} & -2D_0D_1\theta_2 - D_1^2\theta_1 - 2D_0D_2\theta_1 - 2\hat{\mu}_2 D_0\theta_1 - 2c_3 D_0y_1 D_0y_2 - 2c_3 D_0y_1 D_1y_1 \\ & - c_3 y_1 D_0^2 y_2 - c_3 y_2 D_0^2 y_1 - 2c_3 y_1 D_0D_1 y_1 + \frac{\omega_\theta^2}{6}\theta_1^3 + c_4\hat{a}_e\cos\nu t_0\theta_1, \end{aligned} \tag{21}$$

where $D_n = \partial/\partial t_n$. The solution of Eqs. (16) and (17) is written in the form

$$y_1 = A_1(t_1,t_2)\exp(\mathrm{i}t_0) + \overline{A}_1(t_1,t_2)\exp(-\mathrm{i}t_0), \tag{22}$$

$$\theta_1 = A_2(t_1,t_2)\exp(\mathrm{i}\omega_\theta t_0) + \overline{A}_2(t_1,t_2)\exp(-\mathrm{i}\omega_\theta t_0). \tag{23}$$

Substituting Eqs. (22) and (23) into Eqs. (18) and (19), we obtain the condition for the elimination of secular terms in Eqs. (18) and (19) as follows:

$$D_1A_1 + \mathrm{i}\frac{\omega_\theta^2 c_2}{2}\overline{A}_1A_2\exp(\mathrm{i}\hat{\rho}t_1) = 0, \tag{24}$$

$$D_1A_2 + \mathrm{i}\frac{c_3}{\omega_\theta}A_1^2\exp(-\mathrm{i}\hat{\rho}t_1) = 0. \tag{25}$$

Also, substituting Eqs. (22) and (23), and particular solutions of y_2 and θ_2, into Eqs. (20) and (21), we obtain the condition for the elimination of secular terms in Eqs. (20) and (21) as follows:

$$D_2A_1 + \hat{\mu}_1A_1 + c_2\omega_\theta\overline{A}_1(D_1A_2)\exp(\mathrm{i}\hat{\rho}t_1) + \mathrm{i}\left(\frac{5}{3}\alpha_2^2 - \frac{3}{2}\alpha_3 - c_1\right)A_1^2\overline{A}_1 - \frac{\mathrm{i}}{2}D_1^2A_1 - \mathrm{i}\left(\frac{\alpha_2}{2(1-\nu^2)}k_{R1} + \frac{k_{R2}}{2}\right)\hat{a}_e\overline{A}_1\exp(\mathrm{i}\hat{\sigma}t_2) = 0, \tag{26}$$

$$D_2A_2 + \hat{\mu}_2A_2 + \frac{2c_3}{\omega_\theta}A_1(D_1A_1)\exp(-\mathrm{i}\hat{\rho}t_1) - \frac{\mathrm{i}}{2\omega_\theta}D_1^2A_2 + \mathrm{i}\frac{c_2c_3\omega_\theta^2(1+2\omega_\theta)}{2(\omega_\theta^2+2\omega_\theta)}A_1\overline{A}_1A_2 + \frac{\mathrm{i}}{4}\omega_\theta A_2^2\overline{A}_2 = 0. \tag{27}$$

Using transformation

$$A_1 = \frac{1}{2}\hat{a}_1\exp\left(\mathrm{i}\frac{\hat{\sigma}t_2}{2} + \theta_1\right), \quad A_2 = \frac{1}{2}\hat{a}_2\exp(\mathrm{i}(\hat{\sigma}t_2 - \hat{\rho}t_1 + \theta_2)), \tag{28}$$

y and θ are expressed as

$$y = a_1\cos\left(\frac{\nu}{2}t + \theta_1\right) + O(\varepsilon), \tag{29}$$

$$\theta = a_2\cos(\nu t + \theta_2) + O(\varepsilon), \tag{30}$$

where $a_1 = \varepsilon^{1/2}\hat{a}_1$ and $a_2 = \varepsilon^{1/2}\hat{a}_2$. The time variations of the amplitude and phase of the main system and the absorber are governed with the following equations:

$$\frac{\mathrm{d}a_1}{\mathrm{d}t} = -\mu_1a_1 + \frac{c_2\omega_\theta^2\rho}{8}a_1a_2\sin(2\theta_1-\theta_2) - \frac{\omega_\theta^2c_2}{4}a_1a_2\sin(2\theta_1-\theta_2) + \left(\frac{\alpha_2}{2(1-\nu^2)} + \frac{1}{2}k_{R2}\right)a_ea_1\sin2\theta_1, \tag{31}$$

$$\begin{aligned} a_1\frac{\mathrm{d}\theta_1}{\mathrm{d}t} = {} & -\frac{\omega_\theta^2c_2}{4}a_1a_2\cos(2\theta_1-\theta_2) - \frac{\sigma}{2}a_1 - \frac{\omega_\theta^4c_2^2}{32}a_1a_2^2 + \frac{c_2\rho\omega_\theta^2}{8}a_1a_2\cos(2\theta_1-\theta_2) - \frac{1}{8}\left(\frac{10}{3}\alpha_2^2 - 3\alpha_3 - 2c_1 - \left(1+\frac{\omega_\theta}{4}\right)c_2c_3\right)a_1^3 \\ & + \left(\frac{\alpha_2}{2(1-\nu^2)} + \frac{1}{2}k_{R2}\right)a_ea_1\cos2\theta_1, \end{aligned} \tag{32}$$

$$\frac{\mathrm{d}a_2}{\mathrm{d}t} = -\mu_2a_2 + \frac{\rho c_3}{\omega_\theta}a_1^2\cos(2\theta_1-\theta_2) - \frac{c_3}{2\omega_\theta}a_1^2\sin(2\theta_1-\theta_2), \tag{33}$$

$$a_2\frac{\mathrm{d}\theta_2}{\mathrm{d}t} = (\sigma+\rho)a_2 - \frac{c_3}{2\omega_\theta}a_1^2\cos(2\theta_1-\theta_2) - \left(\frac{c_2c_3}{16} + \frac{c_3\omega_\theta}{4} - \frac{c_2c_3\omega_\theta(1+2\omega_\theta)}{8(\omega_\theta^2+2\omega_\theta)}\right)a_1^2a_2 + \frac{\rho c_3}{8\omega_\theta^2}a_1^2\cos(2\theta_1-\theta_2) - \frac{\omega_\theta}{16}a_2^3. \tag{34}$$

For the case $\rho = 0$ ($\omega_\theta = 2$), the steady-state amplitude of the main system and the absorber are analytically expressed as

$$a_{1st} = \sqrt{\frac{12\sigma \pm 24\sqrt{\left(\frac{k_{R2}}{2} + \frac{k_{R1}(k_{R2}-k_{L2})}{2(\nu^2-1)}\right)^2 a_e^2 - \mu_1^2}}{9\alpha_3 - 10\alpha_2^2 + S}}, \tag{35}$$

$$a_{2st} = \left(4c_3 - \frac{7}{4}c_2 c_3\right) a_{1st}, \tag{36}$$

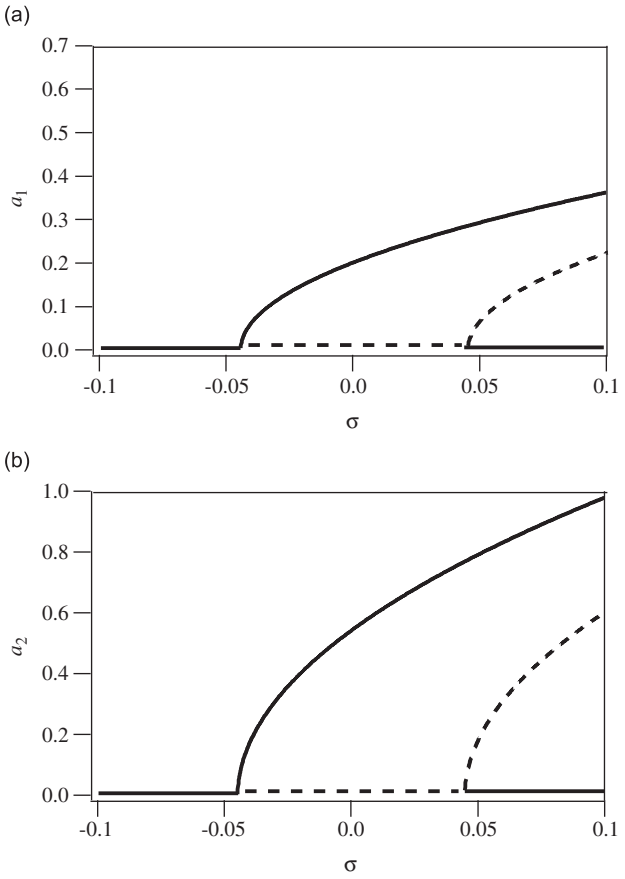

Fig. 3. Frequency response curve in case absorber is in action: (a) main system, (b) absorber: —— stable, – – – unstable.

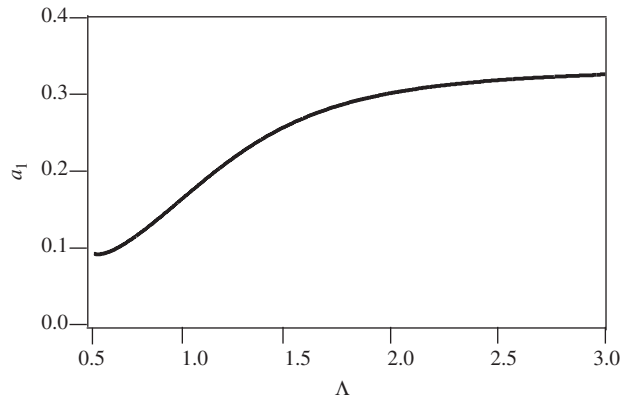

Fig. 4. The influence of length of link on response of the main system.

where $S=6c_1+\frac{3}{2}c_2c_3+48(c_2^2+c_3)-21(c_2^3+c_3)$. From Eqs. (31) and (32), we notice that the absorber affects the motion of the main system. Comparing between Eqs. (10) and (35), the effect of the absorber appears at the denominator in Eq. (35) as the value of S and depends on sign and magnitude of this term. The amplitude of parametric resonance is reduced by the effect of the absorber in the case when S is positive large value.

Fig. 3 shows frequency response curves of the main system and the absorber in the case when the absorber is in action. The solid and broken lines indicate stable and unstable steady-state amplitude, respectively. While the excitation frequency in which parametric resonance occurs is the same as that in Fig. 2, the resonance amplitude of the main system is reduced by the effect of the absorber. For instance, the resonance amplitude of the main system at the excitation

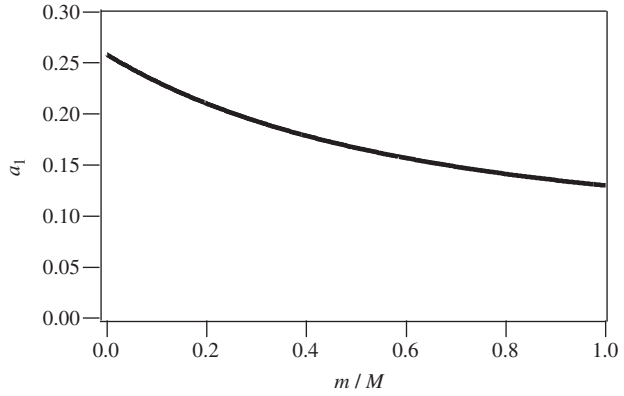

Fig. 5. The influence of mass ratio on response of the main system.

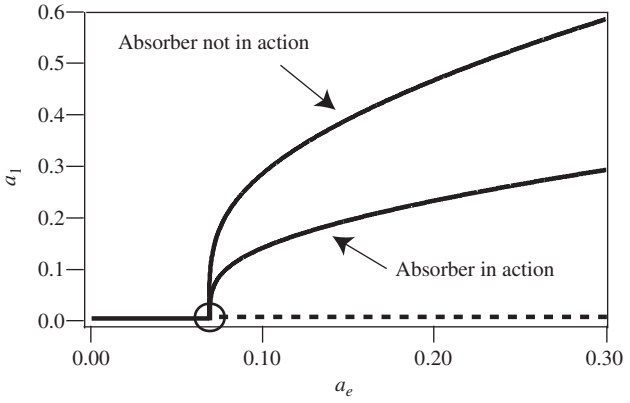

Fig. 6. Force response curves under parametric resonance for the cases that absorber is not in action and in action: —— stable, – – – unstable.

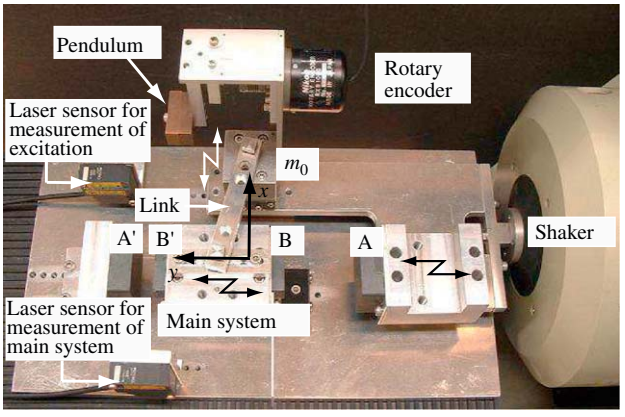

Fig. 7. Picture of experimental setup.

frequency $\nu = 2$ ($\sigma = 0$) in the cases when absorber is not in action and in action, respectively, is 0.34 and 0.20, and the amplitude reduction ratio becomes about 42 percent.

The system parameters which can be changed in the experiment are the length of link Λ and the mass ratio m^* between the main system (mass M) and the absorber in the dimensionless parameters c_1, c_2, and c_3. Fig. 4 shows the influence of length of link on effectiveness of absorber for the case of $m^* = 0.23$ corresponding to the subsequent experimental parameters. As Λ becomes small, the response amplitude of the main system becomes small because S in Eq. (35) becomes large. Fig. 5 shows the influence of the mass ratio m^* for the case of $\Lambda = 1.21$. Also, it can be seen from Eq. (35) that the mass ratio becomes large, the response amplitude of the main system gets smaller. For instance, the response amplitude of

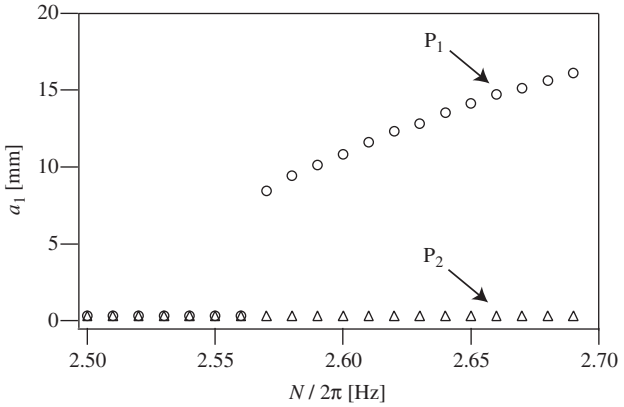

Fig. 8. Experimentally obtained frequency response curve for the cases that absorber is not in action and in action: circle is in case absorber is not in action, triangle is in case absorber is in action.

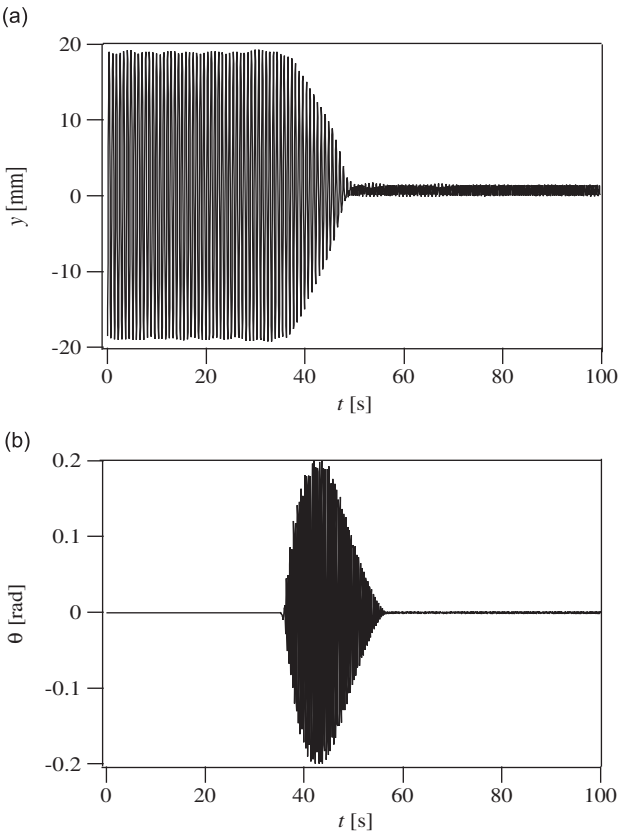

Fig. 9. Time histories in case absorber is in action when excitation frequency is 2.66 Hz: (a) main system, (b) absorber.

the main system for the case of $\Lambda = 0.9$ in Fig. 4 is reduced from 0.34 to 0.13 about 62 percent, and for the case of $m/M = 0.5$ in Fig. 5 is reduced from 0.34 to 0.16 about 53 percent.

In Fig. 6, we show variations of the amplitude of the main system $a_1 (= \varepsilon^{1/2}\hat{a}_1)$ and the absorber $a_2 (= \varepsilon^{1/2}\hat{a}_2)$ with excitation amplitude a_e. The solid and dashed line, respectively, represent stable and unstable steady-state amplitude. The upper and lower lines, respectively, indicate the response amplitude of the main system in the cases when absorber is not in action and in action. As a_e increases from zero to the circle ($a_e = 0.069$), parametric resonance does not occur, and supercritical pitchfork bifurcation happens at the circle. The amplitude of parametric resonance is reduced by the effect of the absorber in all excitation amplitude.

3. Experimental results

We show the experimental apparatus in Fig. 7. The main system M, which is subjected to repulsive magnetic forces from both sides, can move freely in the y-direction on a slide bearing that is mounted on the horizontal plane. We move magnet A in the y-direction as $y_0 = a_e \cos Nt$ by an electromagnetic shaker (Type 513-B; EMIC Corp). A mass m_0 is connected to the main system by a link; it can move freely in the x-direction. The motions of magnet A and the main system are measured using laser displacement sensors (LB-01; Keyence Corp).

A pendulum with tip mass m, whose natural frequency is tuned to be twice that of the main system, is supported by a radial bearing. The angle is measured using a rotary encoder (RXB1000; Nikon Corp). By the connection between the absorber and the main system by the link, the pendulum of the absorber is excited with twice the response frequency of the motion of the main system.

The dimensions of magnets A and A' are $50 \times 50 \times 18$ mm, and the dimensions of B is $40 \times 20 \times 10$ mm and B' is $40 \times 40 \times 10$ mm. The dimensions for the main system and the absorber are as follows: $y_{st} = 33$ mm, $M = 0.562$ kg, $m_0 = 0.25$ kg, $m = 0.13$ kg, $a_e = 40$ mm, $L = 40$ mm, $l = 32$ mm, $l_M = 182$ mm, $l_0 = 100$ mm. The natural frequencies of the main system and the absorber are $\Omega_y/2\pi = 1.33$ Hz, and $\Omega_\theta/2\pi = 2.66$ Hz, respectively.

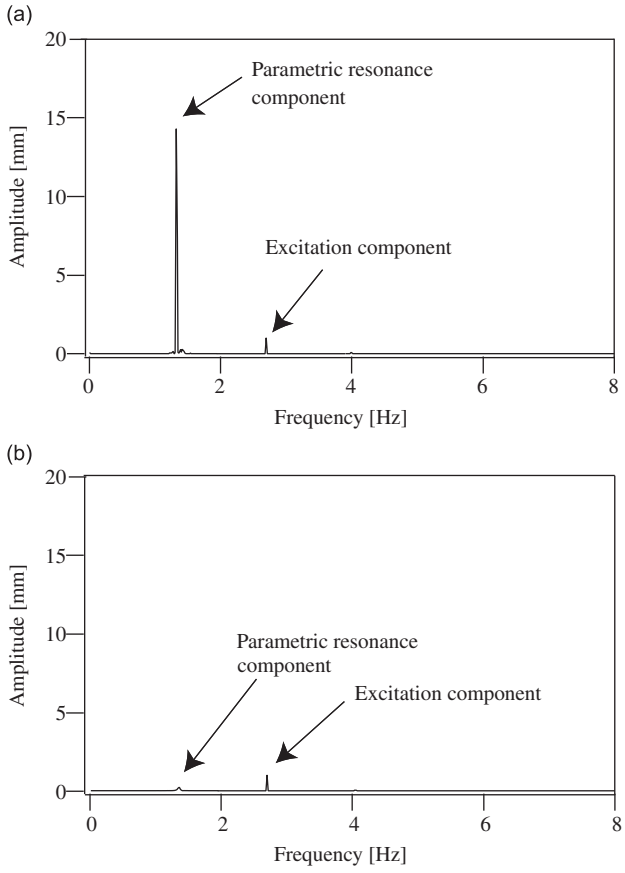

Fig. 10. Spectral analysis of the main system: (a) in case absorber is not in action, (b) in case absorber is in action.

3.1. Experimental bifurcation diagram and the effect of Coulomb friction

Fig. 8 shows frequency response curves of the parametric resonance in the case when absorber is not in action (absorber is mechanically fixed by bolt) and in action (absorber is released from fixation). Circles indicate the steady-state amplitude in the case that absorber is not in action and triangles indicate the steady-state amplitude in both cases that absorber is in action and not in action. In this section, we discuss the case that absorber is not in action.

In the case of $N/2\pi > 2.57$ Hz, there are two stable steady-state amplitude; one is zero amplitude denoted by triangles, and the other one is finite amplitude denoted by circles in the state where parametric resonance is produced. Hence, depending on the magnitude of initial condition or disturbance, parametric resonance is produced, regardless of Coulomb friction acting on the main system due to the slide bearing.

However, the response amplitude of the main system below excitation frequency $N/2\pi = 2.57$ Hz in the case when absorber is not in action becomes suddenly close to zero and the response amplitude below 8 mm in this experimental

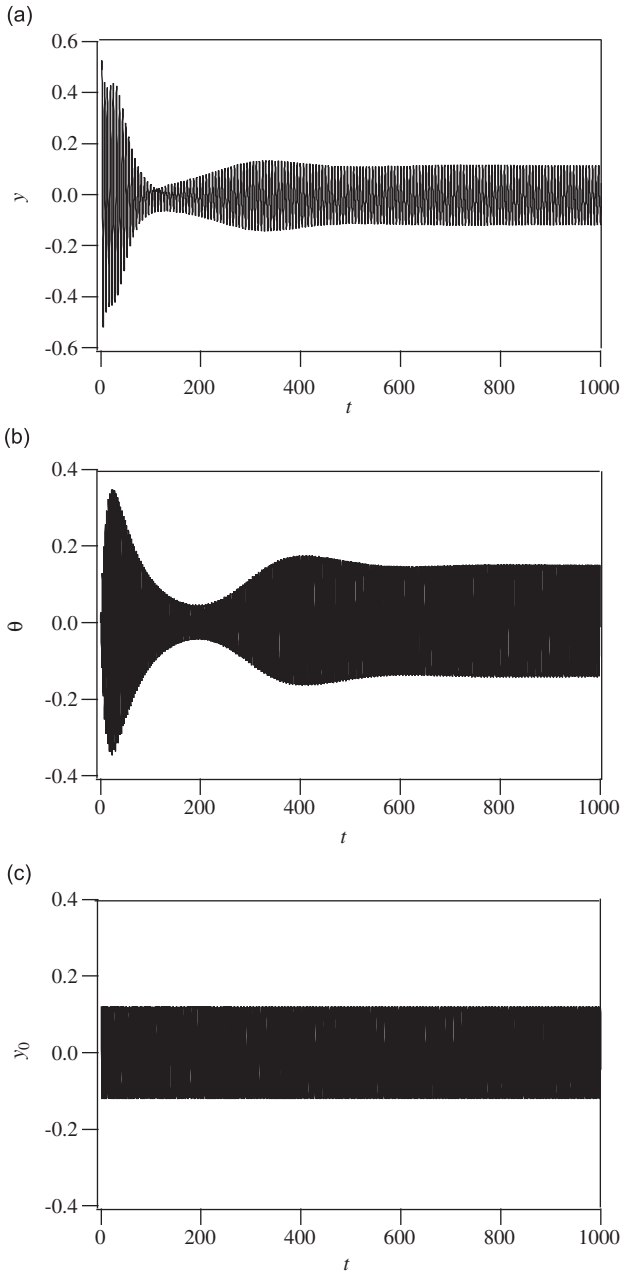

Fig. 11. Time histories in the case when absorber is in action ($y(0) = 0.5$, $\dot{y}(0) = 0.2$): (a) main system, (b) absorber, (c) excitation.

apparatus is not observed. This difference between Fig. 8 and the analytical result in Fig. 2 may be due to the reason why the analytical approach does not consider the Coulomb friction. It is numerically examined later that both effect of the Coulomb friction acting on the main system and action of the absorber reduce the amplitude of the parametrically excited main system to zero.

3.2. Stabilization of parametric resonance

Fig. 9 shows experimentally obtained time histories of the main system and the absorber in the case when absorber is not in action and in action. At $t \approx 30$ s, the absorber is released from fixation and is excited by the motion of the main system. Then, the response amplitude of the main system becomes close to zero. As seen from Fig. 9(b), the absorber works only in the transient state after the release where the main system changes the steady-state amplitude from finite

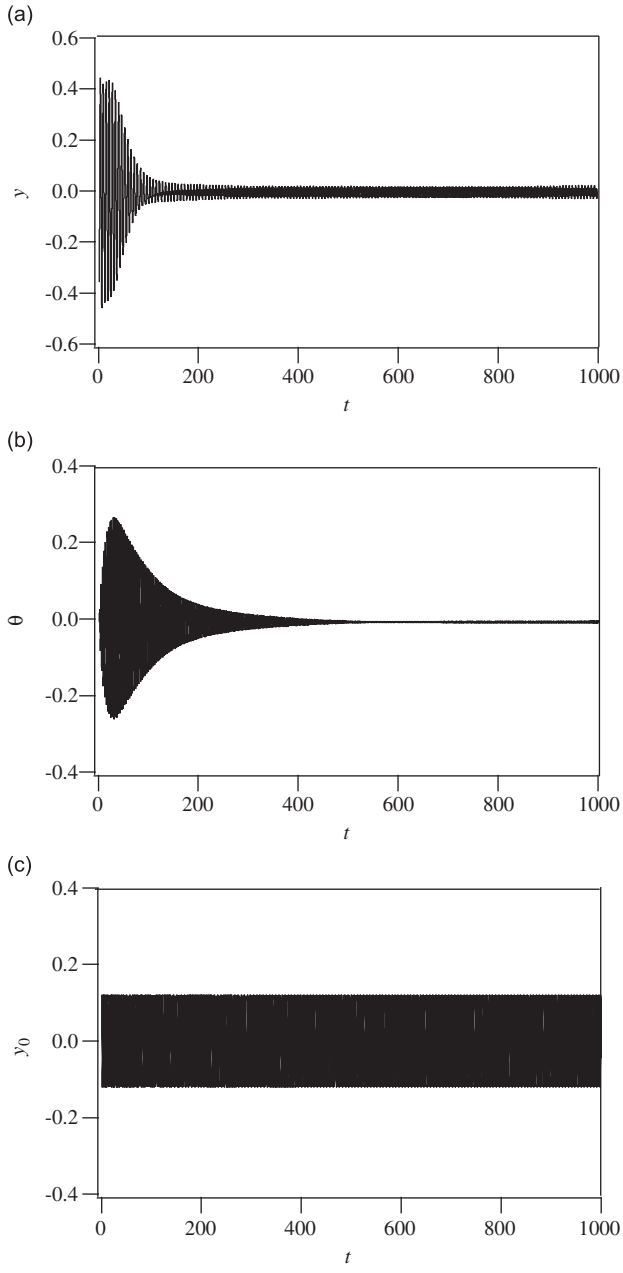

Fig. 12. Time histories in the case when absorber is in action with Coulomb friction ($y(0) = 0.5$, $\dot{y}(0) = 0.2$): (a) main system, (b) absorber, (c) excitation.

magnitude to the trivial one (zero amplitude). If the absorber is not released, the parametric response is kept also after $t \approx 30$ s.

Fig. 10 shows experimentally obtained spectral analyses of the main system. Fig. 10(a) and (b) show the cases that the absorber is not in action and in action, respectively. P_1 in Fig. 8 is the amplitude in the interval of 0–30 of time history in Fig. 9(a) and Fig. 10(a) is the spectral analysis in that period. P_2 in Fig. 8 is the amplitude in the interval of 60–80 of that in Fig. 9(b) and Fig. 10(b) is the spectral analysis in that period. The magnitude of the frequency component due to the parametric resonance remarkably decreases in spectral analysis.

When the main system is stabilized, the amplitude of the absorber is zero. The absorber does not act in a way as to counter the sinusoidal excitation. The excitation externally keeps to excite the main system through the first term in the right hand side of Eq. (4). However, because the excitation frequency is far from the linear natural frequency, the response amplitude is very small. The frequency component is experimentally observed as the excitation component in Fig. 10(b).

3.3. Stabilization mechanism for main system subjected to Coulomb friction

As shown in Fig. 3, the amplitude is reduced, but is not close to zero in the analytical result without considering Coulomb friction. In experiment, it appears that the almost suppression is carried out by inherently existing Coulomb friction in the main system, in addition to the effect of the absorber. In order to examine the influence of small Coulomb friction, which inherently exists in main system, we numerically analyze it using Runge–Kutta method (analytical approach for parametrically excited system subjected to Coulomb friction is an open problem, while an analytical approach for self-excited system subjected to Coulomb friction is proposed in [16]).

The results are obtained by integrating Eq. (11) including the term of $f_k(\dot{y})$ where f_k denotes magnitude of Coulomb friction [17]. The magnitude of Coulomb friction in experiment is 0.002. Figs. 11 and 12 show time histories of the main system, absorber, and excitation, and Fig. 13 shows spectrum analyses of the main system. Figs. 11 and 13(a) represent the case that absorber is in action and the Coulomb friction is not considered. The resonance amplitude of the main system is reduced by the effect of the absorber but cannot be minimized as analytically predicted without considering Coulomb friction in Section 2.3. Figs. 12 and 13(b) represent the case that absorber is in action and the Coulomb friction is considered. Parametric resonance of the main system is minimized by the effect of both the absorber and the Coulomb

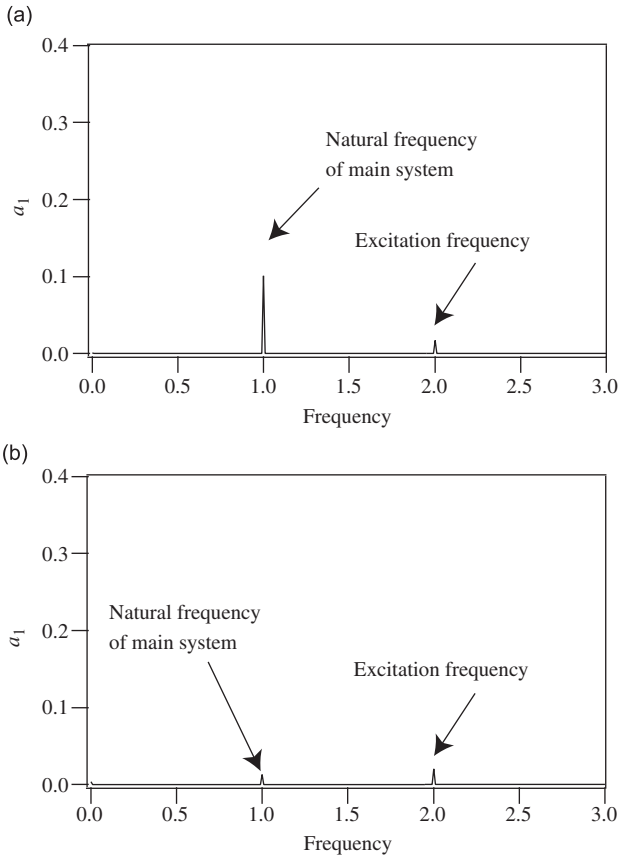

Fig. 13. Numerical analysis of spectrum: (a) without considering Coulomb friction, (b) considering Coulomb friction.

friction. The absorber works to reduce the response amplitude in the range where the nontrivial steady-state amplitude does not exist due to the Coulomb friction, i.e., below 8 mm in the previous experiment. As a result, the parametric resonance is stabilized to be zero amplitude.

4. Conclusions

In this paper, we have discussed the amplitude reduction method of parametric resonance using a nonlinear dynamic vibration absorber. This method utilizes quadratic nonlinear coupling between the main system and the absorber, where the absorber is not autoparametrical but externally excited. To realize such a nonlinear coupling, we connect geometrically a pendulum, whose natural frequency is twice the natural frequency of the main system, with the main system. Analytical results using the method of multiple scales, numerical results using Runge–Kutta method, and experimental results show that the proposed absorber is effective in reducing parametric resonance amplitude. The detail results are summarized as follows:

(1) Analytical results show that the amplitude of the parametric resonance is reduced by the effect of the proposed vibration absorber, whose natural frequency is twice that of the main system.
(2) Experimental results show that steady-state amplitude of the parametric resonance becomes close to zero by the absorber. The stabilization is carried out by both effects of the proposed absorber and the Coulomb friction acting on the main system.
(3) System parameters which influence on effectiveness of the absorber are length of the link and mass ratio between the main system (mass M) and the absorber. As length of the link becomes small and mass ratio becomes large, the effectiveness of the absorber becomes large.

References

[1] A.H. Nayfeh, D.T. Mook, *Nonlinear Oscillations*, Wiley, New York, 1979.
[2] B. Pratiher, S.K. Dwivedy, Parametric instability of a Cantilever beam with magnetic field and periodic axial load, *Journal of Sound and Vibration* 305 (2007) 904–917.
[3] B.W. Huang, J.H. Kuang, The parametric resonance instability of a drilling process, *Transactions of the ASME Journal of Applied Mechanics* 74 (2007) 958–964.
[4] G. Shaw, R. Baskaran, Tunable microelectromechanical filters that exploit parametric resonance, *Transactions of the ASME Journal of Vibration and Acoustics* 127 (2005) 423–430.
[5] S.W. Piccardo, F. Tubino, Parametric resonance of flexible footbridges under crowd-induced lateral excitation, *Journal of Sound and Vibration* 311 (2008) 353–371.
[6] J.P. Racz, J.F. Scott, Parametric instability in a rotating cylinder of gas subjected to sinusoidal axial compression, *Journal of Fluid Mechanics* 595 (2008) 265–290.
[7] G. Mustafa, A. Ertas, Dynamics and bifurcations of a coupled column-pendulum oscillator, *Journal of Sound and Vibration* 182 (1995) 393–413.
[8] H. Yabuno, T. Murakami, J. Kawazoe, N. Aoshima, Suppression of parametric resonance in cantilever beam with a pendulum (effect of static friction at the supporting point of the pendulum), *Transactions of the ASME Journal of Vibration and Acoustics* 26 (2004) 149–162.
[9] W. Lacarbonara, C.M. Chin, R.R. Soper, Open-loop nonlinear vibration control of shallow arches via perturbation approach, *Transactions of the ASME Journal of Applied Mechanics* 69 (2002) 325–334.
[10] R.S. Haxton, A.D.S. Barr, The autoparametric vibration absorber, *Transactions of the ASME Journal of Engineering for Industry* 94 (1972) 119–125.
[11] O. Cuvalci, The effect of detuning parameters on the absorption region for a coupled system: a numerical and experimental study, *Journal of Sound and Vibration* 229 (2000) 837–857.
[12] A. Vyas, A. Bajaj, A. Raman, Dynamics of structures with wideband autoparametric vibration absorber: theory, *Proceedings of the Royal Society of London A* 460 (2004) 1547–1581.
[13] H. Yabuno, R. Kanda, W. Lacarbonara, N. Aoshima, Nonlinear active cancellation of the parametric resonance in a magnetically levitated body, *Transactions of the ASME Journal of Dynamic, Systems, Measurement, and Control* 126 (2004) 433–442.
[14] H. Jo, H. Yabuno, Parametric resonance due to asymmetric nonlinearity of restoring force, *Journal of System Design and Dynamics* 2 (2008) 893–907.
[15] H. Jo, H. Yabuno, Amplitude reduction of primary resonance of nonlinear oscillator by a dynamic vibration absorber using nonlinear coupling, *Nonlinear Dynamics* 55 (2009) 67–78.
[16] H. Yabuno, Y. Kunitho, T. Kashimura, Analysis of the van der Pol system with coulomb friction using the method of multiple scales, *Transaction of ASME Journal of Vibration and Acoustics* 130 (2008) 041008-1–041008-7.
[17] B.F. Feeny, J.W. Liang, A decrement method for the simultaneous estimation of coulomb and viscous friction, *Journal of Sound and Vibration* 195 (1996) 149–154.